JOC The Journal of Organic Chemistry

Article

pubs.acs.org/joc

A Musclelike [2](2)Rotaxane: Synthesis, Performance, and Molecular Dynamics Simulations

Hong Li,[†] Xin Li,[‡] Ying Wu,[†] Hans Ågren,[‡] and Da-Hui Qu*[,†]

[†]Key Laboratory for Advanced Materials and Institute of Fine Chemicals, East China University of Science & Technology, Shanghai 200237, People's Republic of China

[‡]Division of Theoretical Chemistry and Biology, School of Biotechnology, KTH Royal Institute of Technology, SE-10691 Stockholm, Sweden

Supporting Information

ABSTRACT: A novel bistable symmetric [2](2)rotaxane was prepared by a threading-followed-by-stoppering strategy and characterized with ^{1}H, ^{13}C, and 2D ROESY NMR spectroscopy and HR-ESI spectrometry. The symmetric [2](2)rotaxane system consists of an anthracene-based bis(crown ether) as macrocycles, and each of the two dibenzo[24]crown-8 (DB24C8) rings is threaded by the pendant substituents of a symmetrically substituted central rotatable ferrocene subunit that possesses two distinguishable recognition sites for the DB24C8 ring: namely, a dibenzylammonium site and an *N*-methyltriazolium site. The uniform shuttling motion of the thread relative to the two DB24C8 rings in [2](2)rotaxane can be driven by external acid−base stimuli, which was evidenced by ^{1}H and 2D ROESY NMR spectroscopy. Furthermore, molecular dynamics simulations of the [2](2)rotaxane were carried out both in protonated (stretched) and in neutral (contracted) forms. The calculated percentage change in molecular length of the [2](2)rotaxane between the two end-capping bis(methoxyl)phenyl groups is about 48% in the two different states (in acetone), which is much larger than the percentage change (~27%) in human muscle. Moreover, in the two states, the C*−Cp−Cp−C* dihedral angles are computed as −177° in the stretched state and −112° in the contracted state, indicating a correlation between the translational and rotational motions of the [2](2)rotaxane.

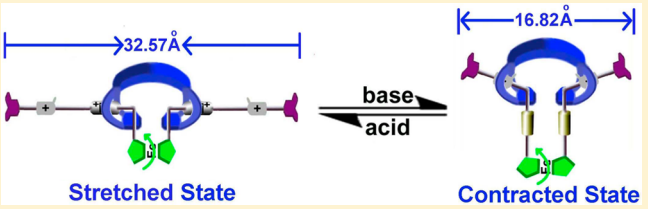

INTRODUCTION

In the past few decades, the fascinating biological motors and macroscopic machines have become the sources of inspiration for chemists to design various artificial molecular machines.[1] The key theme in the field of artificial molecular machines is to design molecules with addressable structure in order to control molecular motion by applying external stimuli.[2] Rotational and translational motions, which are the two most common and fundamental movements, have been successfully performed with a variety of linear motors[3] and rotary motors.[4] Among linear motors, of special interest is the class of molecular muscles, which are delicately controlled linear machines exhibiting reversible, programmed contraction and stretching movements.[5] The structure of these muscles is generally based on mechanically interlocked molecules (MIMs)[1,6] containing mobile structural elements that are able to move with respect to one another upon external stimulus. The externally induced reversible contraction and extension of such molecular structures is a mimic of the movement of skeletal muscle. MIMs, in particular bistable rotaxanes, have been employed not only as the basis of molecular muscles but also as molecular shuttles,[7] molecular elevators,[8] molecular information ratchets,[9] molecular synthetic machines,[10] and so on. Recently, [2](2)rotaxane, a two-component interlocked molecular system that has two threadings involved, has been used to construct a nanoscale molecular elevator[8] or to mimic the flapping wings of a butterfly.[11] However, the potential of the [2](2)rotaxane system to behave as a molecular muscle on the basis of the combination of rotational and translational motion in a single molecular system still remains unexplored.

Herein, we report the design and synthesis of the novel bistable [2](2)rotaxane **1** (Scheme 1), which can mimic the stretching and contractional motion performed by skeletal muscle, accompanied by a molecular rotary motion. As shown in Scheme 1, the [2](2)rotaxane system has a symmetric structure, which contains an anthracene-based bis(dibenzo[24]-crown-8) (bis-DB24C8) as macrocycles,[12] and each of the two macrocycles is threaded by the pendant substituents of a symmetrically substituted central rotatable ferrocene (Fc) unit.[13] The two identical substituents of the ferrocene possess two distinguishable recognition stations: namely, a predominant dibenzylammonium (DBA)[14] site and a secondary *N*-methyltriazolium (MTA)[15] site. Applying ^{1}H NMR and 2D ROESY NMR spectroscopy and molecular dynamics simulations, we have shown that external acid−base stimuli can result in a reversible stretching and contractional mechanical motion of the system, in which the percentage change of the molecular length is around 48%, which is much larger than that of the human muscle (~27%). Moreover, the musclelike motion is

Received: May 22, 2014
Published: July 16, 2014

   dx.doi.org/10.1021/jo501127h | J. Org. Chem. 2014, 79, 6996−7004

Scheme 1. Switching Process and the Schematic Representation of the Novel Bistable [2](2)Rotaxane 1 That Can Switch between Two Different States

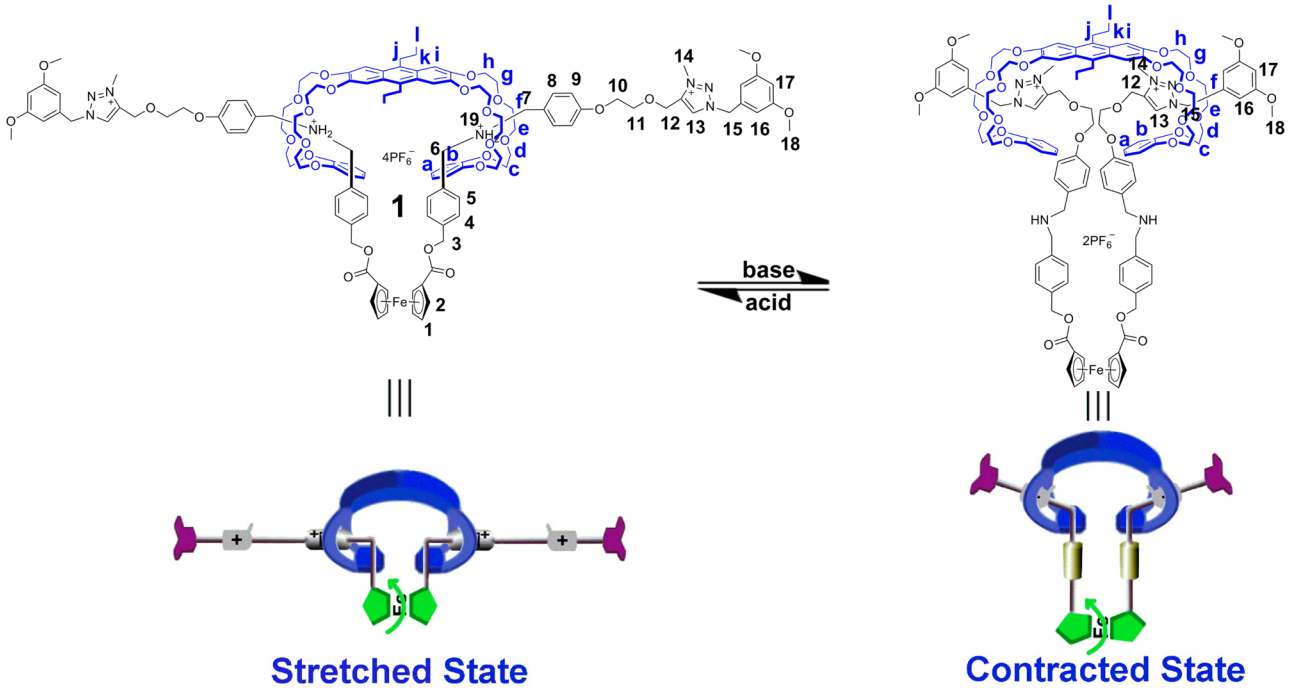

accompanied by a rotational motion of the ferrocene unit, indicating that the system can perform coupled mechanical motions. These results can pave the way for the design and construction of more complicated molecular machines.

RESULTS AND DISCUSSION

Molecular Design and Syntheses. The syntheses, chemical structures, and model diagrams of [2](2)rotaxanes **1** and **2** and compound **3**, as well as two key intermediates, i.e., the ferrocene-containing bis-branched precusor **7** and anthracene-based bis(dibenzo[24]crown-8) **8**, are shown in Scheme 2 and Schemes S1 and S2 (see the Supporting Information).

As shown in Scheme 2, the mixture of guest **7** and host **8**[12] in a 1:1 molar ratio form predominantly [2](2)pseudorotaxane in CH_2Cl_2. A subsequent "click" reaction with the stopper azide **9** in the presence of the catalyst $Cu(CH_3CN)_4PF_6$ gives [2](2)rotaxane **2** in 42% yield. The secondary recognition site MTA stations for DB24C8 were introduced by treating [2](2)rotaxane **2** with CH_3I at room temperature followed by anion exchange with saturated NH_4PF_6, giving the target [2](2)rotaxane **1** in a good yield (64%). The synthesis of reference compound **3** is shown in Scheme S2 (see the Supporting Information). The [2](2)rotaxanes **1** and **2**, compound **3**, and the key intermediate compound guest **7** were all characterized by ^1H and ^{13}C NMR spectroscopy and high-resolution electrospray ionization (HR-ESI) mass spectrometry. The reversible acid−base-driven mechanical movement of [2](2)rotaxane **1** was also investigated by ^1H NMR and 2D ROESY spectroscopy.

The HR-ESI mass spectra provided evidence for the formation of the [2](2)rotaxanes **1** and **2**, which had signals at m/z 1299.4982 and 1139.9967 as single charged peaks for $[M - 2PF_6]^{2+}$, respectively. The HR-ESI mass spectrum also confirmed the structure of compound **3** having the most intense peak at m/z 1741.4650 as a singly charged peak for $[M - PF_6]^+$.

^1H NMR Measurements. The ^1H NMR spectra (Figure 1) of [2](2)rotaxane **1**, compound **3**, and anthracene-based bis-DB24C8 macrocycle host **8** in CD_3CN showed that the DB24C8 macrocycle encircled at the DBA recognition site in the structure of [2](2)rotaxane **1**. In comparison to those of host **8** (Figure 1a), the peaks for the phenyl protons H_i on the anthracene moiety of [2](2)rotaxane **1** (Figure 1b) were shifted upfield with a $\Delta\delta$ value of −0.30 ppm, while the alkyl protons H_j, H_k and H_l showed no apparent changes (for the location of the discussed H atoms within the structures, see Scheme 1). These results are attributed to the shielding effect of the ferrocene on the anthracene moiety after the self-assembly of guest **7** and host **8**. Comparison of the chemical shifts of the H atoms of compound **3** before and after assembly (Figure 1c vs Figure 1b) shows some considerable changes. For instance, the phenyl protons H_5 and H_8 adjacent to the DBA site were shifted upfield with $\Delta\delta$ values of −0.21 and −0.50 ppm, respectively. The protons H_2 and H_1 on the Cp rings of Fc were also shifted upfield with $\Delta\delta$ values of −0.31 and −0.14 ppm, respectively. More interestingly, the methylene protons H_6 and H_7 on the DBA station were obviously shifted downfield with $\Delta\delta$ values of 0.72 and 0.65 ppm, giving two broad absorptions in comparison to the two sharp singlets in compound **3**, respectively. Moreover, it was notable that the central ammonium hydrogen atoms (NH_2^+) H_{19} in [2](2)rotaxane **1** were detected, which resulted from the stabilizing effect of the hydrogen-bonding interactions between the DB24C8 and the NH_2^+. In other words, the fact that the NH_2^+ H_{19} hydrogen atoms in compound **3** did not appear suggested the exclusion of the central ammonium sites by the DB24C8 ring in compound **3**. Additionally, the 2D ROESY NMR spectrum of [2](2)rotaxane **1** (Figure 2a) in CD_3COCD_3 showed clear correlation peaks between the methylene protons H_j and H_k on the DB24C8 macrocycle and the phenyl protons H_4 (peak A), H_9 (peak D), and the alkyl protons H_6, H_7 (peak E) on the thread near the DBA recognition sites. An especially remarkable

dx.doi.org/10.1021/jo501127h | J. Org. Chem. 2014, 79, 6996−7004

Scheme 2. Preparation of Target [2](2)Rotaxanes 1 and 2 and the Chemical Structure of Compound 3

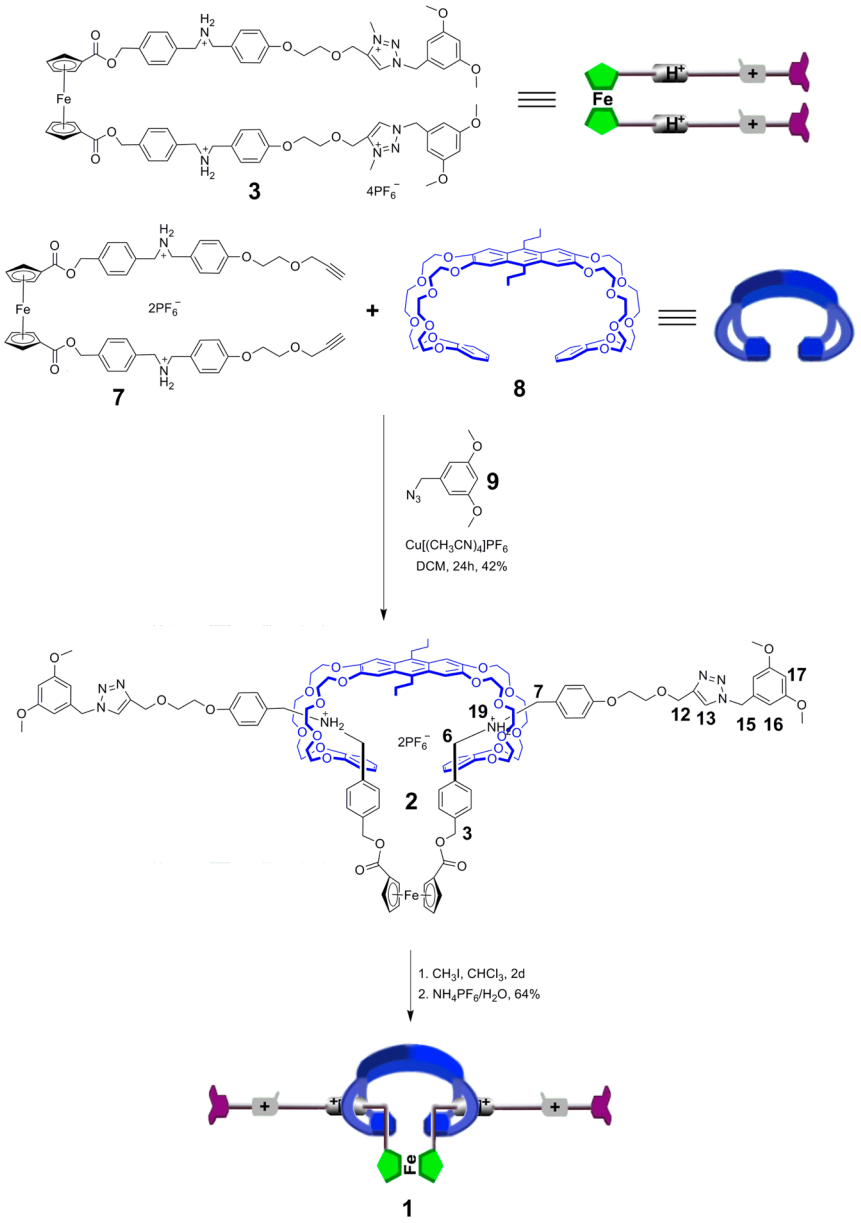

correlation peak (peak F) between the phenyl protons H_4 on the rod part adjacent to ferrocene and phenyl protons H_a on the crown ether macrocycle suggested a $\pi-\pi$ interaction between the phenyl rings close to one Cp ring and the aromatic units in the crown ether macrocycle. All of these spectroscopic results are evidence that the bis-DB24C8 macrocycle is encircled at the DBA recognition site in the structure of [2](2)rotaxane **1**.

The reversible acid–base-driven shuttling motion of the macrocycle between the two distinguishable recognition sites in the system of [2](2)rotaxane **1** was also investigated using ^{1}H NMR spectroscopy (Figure 3). The macrocycle was moved to the MTA recognition site from the original DBA recognition site by deprotonation of the DBA moiety upon addition of 2.0 equiv of 1,8-diazabicyclo[5.4.0]undec-7-ene (DBU) to the CD_3COCD_3 solution of [2](2)rotaxane **1**. This structural change is accompanied by remarkable ^{1}H NMR spectral changes. As shown in Figure 3b, the protons H_{13} and H_{14} on the MTA station were shifted by $\Delta\delta$ values of 0.67 and −0.42 ppm, respectively, while the methylene protons H_6 and H_7 on the DBA station were shifted upfield ($\Delta\delta$ = −0.72 ppm). Furthermore, the phenyl protons H_i on the anthracene moiety and H_2 and H_1 on the Cp rings of Fc were all shifted downfield ($\Delta\delta$ = 0.14, 0.18, and 0.07 ppm, respectively). The shifts are diagnostic of the movement of the bis-DB24C8 macrocycle to the MTA recognition site upon the addition of 2.0 equiv of DBU. Furthermore, the 2D ROESY NMR spectrum of the DBU-added [2](2)rotaxane **1** (Figure 2b) also provided good evidence for the fact that the bis-DB24C8 ring was encircled on the MTA station. Crucially, the ^{1}H NMR spectrum of the DBU-added [2](2)rotaxane **1** could be regenerated to the original ^{1}H NMR spectrum by reprotonation of the dibenzylamine center upon addition of 4.0 equiv of CF_3COOH (TFA) (Figure 3c). This indicated that the bis-DB24C8 macrocycle was completely repositioned to the DBA sites. The shuttling motion between the two distinguishable recognition sites is reversible using repeated base (DBU) and acid (TFA) addition cycles.

dx.doi.org/10.1021/jo501127h | J. Org. Chem. 2014, 79, 6996–7004

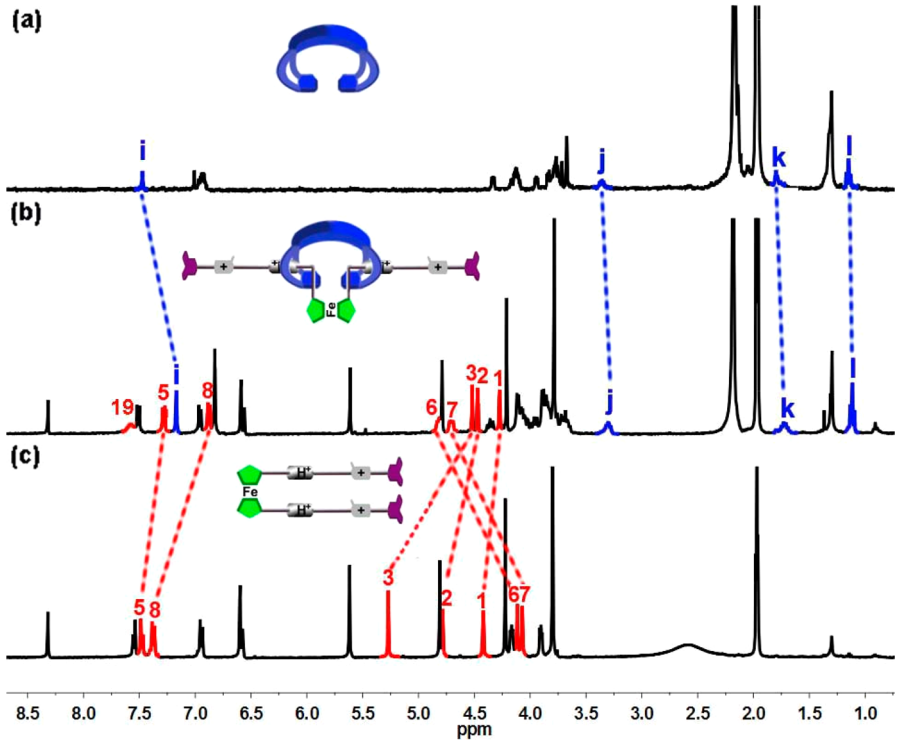

Figure 1. ^{1}H NMR spectra (400 MHz, CD_3CN, 2.0×10^{-3} M, 298 K) of (a) host **8**, (b) [2](2)rotaxane **1**, and (c) compound **3**. The assignments correspond to the structures shown in Scheme 1.

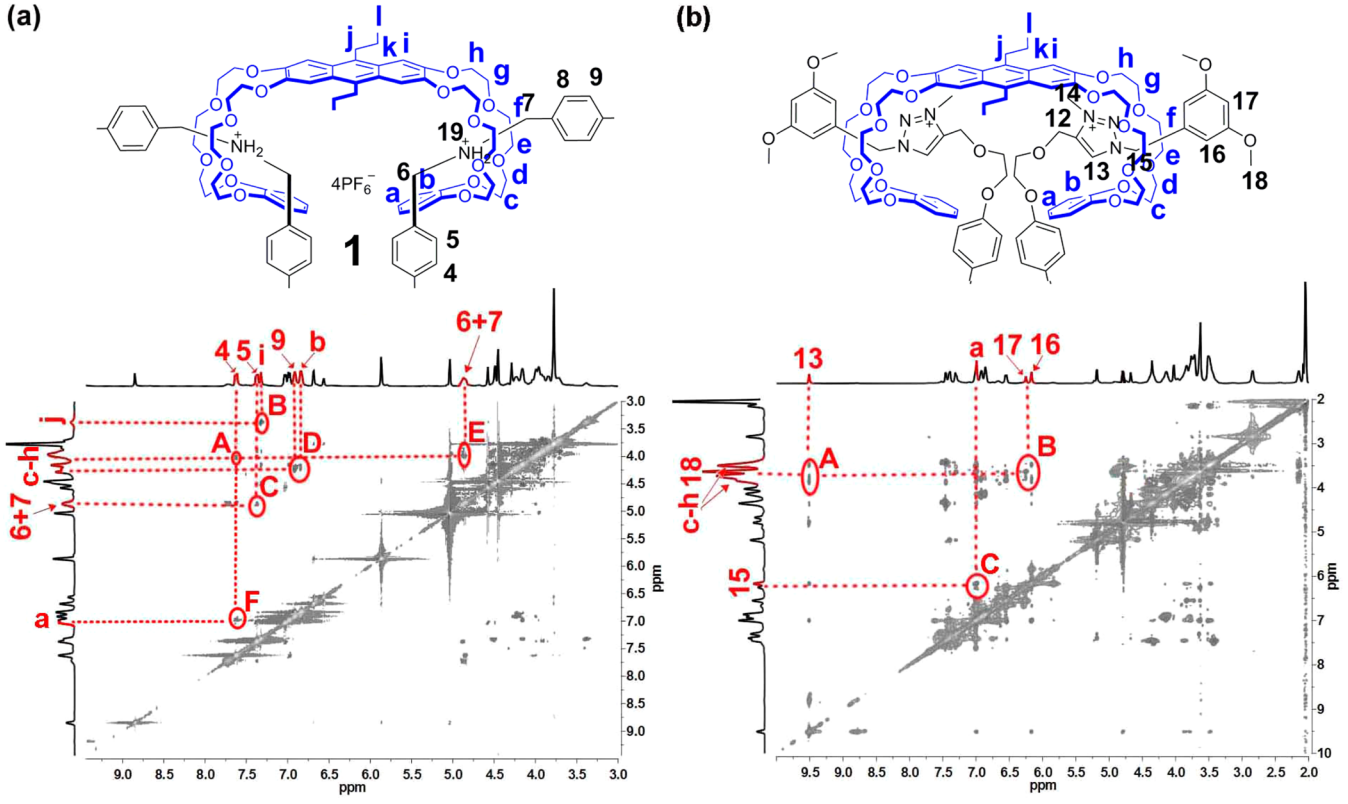

Figure 2. Partial 2D ROESY NMR spectrum (400 MHz, CD_3COCD_3, 2.0×10^{-3} M, 298 K) of (a) [2](2)rotaxane **1** and (b) upon addition of 2.0 equiv of DBU to (a).

Molecular Dynamics Simulations of [2](2)Rotaxane 1 in Different States. To gain insights into the structural differences in the two states, we carried out theoretical simulations of different states of the [2](2)rotaxane **1** at 298 K in acetone for 10 ns. With the optimized geometries as starting points, molecular dynamics (MD) simulations were conducted employing

dx.doi.org/10.1021/jo501127h | J. Org. Chem. 2014, 79, 6996−7004

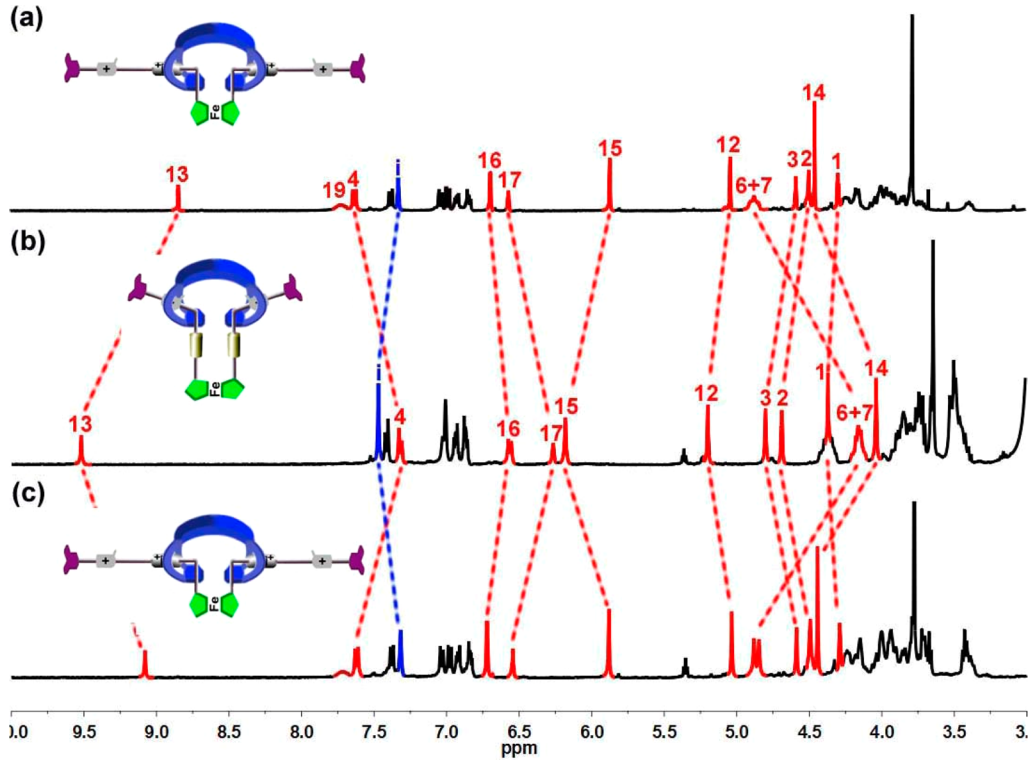

Figure 3. Partial ^{1}H NMR spectra (400 MHz, CD_3COCD_3, 2.0 × 10^{-3} M, 298 K) of (a) [2](2)rotaxane **1**, (b) deprotonation with addition of 2.0 equiv of DBU to (a), and (c) reprotonation with addition of 4.0 equiv of TFA to (b). The assignments correspond to the structures shown in Scheme 1.

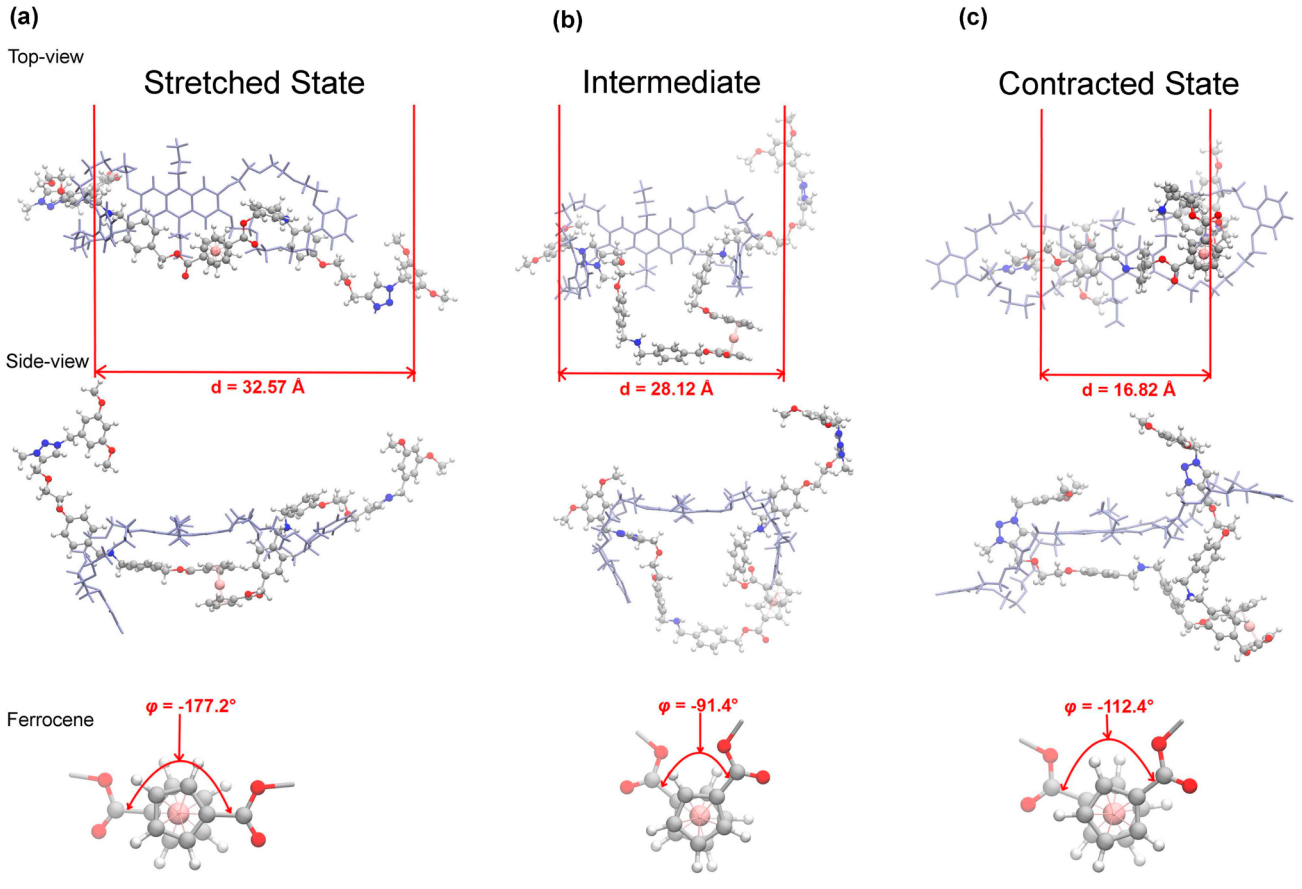

Figure 4. Snapshots for the structures of the [2](2)rotaxane **1** at different states, extracted from MD trajectories in acetone.

dx.doi.org/10.1021/jo501127h | J. Org. Chem. 2014, 79, 6996−7004

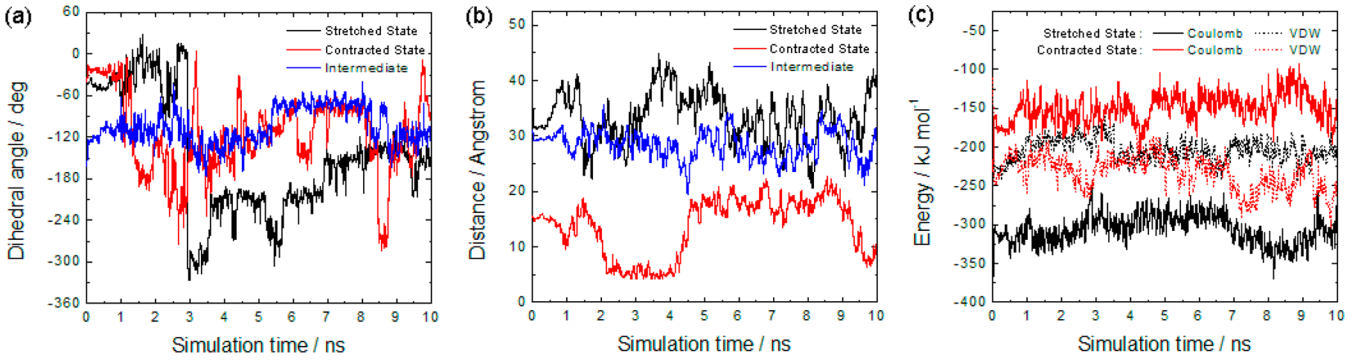

Figure 5. (a) Dihedral angle C*−Cp−Cp−C* of the [2](2)rotaxane **1** in acetone. (b) Distance between the two end-capping bis(methoxyl)phenyl groups of the [2](2)rotaxane **1** in acetone. (c) Interaction energy between the ferrocene-containing dumbbell and the crown ether macrocycle of the [2](2)rotaxane **1** in acetone.

Table 1. C*−Cp−Cp−C* Dihedral Angle of Ferrocene, End-to-End Distance of the Dumbbell, Distance between the Fe(II) Center and the Anthracene Unit, and Interaction Energy between the Dumbbell and the Macrocycle in Acetone[a]

			$d_{Fe-anthracene}$/Å		$E_{interaction}$/kJ mol^{-1}	
	$\varphi_{C^*-Cp-Cp-C^*}$/deg	$d_{end\text{-}to\text{-}end}$/Å	site 9	site 10	Coulomb	VDW
stretched state	−177.2 ± 41.4	32.57 ± 4.39	6.72 ± 0.69	7.58 ± 1.33	−307.9 ± 22.0	−207.1 ± 13.8
contracted state	−112.4 ± 50.4	16.82 ± 3.56	14.03 ± 1.18	13.31 ± 1.51	−142.3 ± 19.8	−242.9 ± 22.5
intermediate	−91.4 ± 26.1	28.12 ± 2.91	13.56 ± 1.05	12.68 ± 1.20	−259.1 ± 16.2	−214.9 ± 16.5

[a]Each quantity is listed as an average over the last 5 ns of simulation trajectory together with its standard deviation.

the general Amber force field[16] in combination with the parameters for ferrocene developed by Lopes et al.[17] Snapshots for the [2](2)rotaxane **1** at different states are shown in Figure 4. It can be seen that, in the stretched state (Figure 4a), both amine groups are protonated, and the ferrocene-based dumbbell exhibits a stretched conformation to facilitate interaction between the crown ether macrocycle and the ammonium ions. The two phenyl rings adjacent to ferrocene are also found to show $\pi-\pi$ interaction with the aromatic units in the crown ether macrocycle. In the contracted state (Figure 4c), both amine groups are neutral and the ferrocene-containing dumbbell adopts a contracted conformation with its two arms intertwined with each other, in order to facilitate interaction between the crown ether macrocycle and the triazolium ions. Thus, the interconversion between a stretched state and a contracted state corresponds to the stretching and contraction of the ferrocene-containing dumbbell. The intermediate state, where only one amine group is protonated, shows a half-contracted conformation (Figure 4b). Interestingly, the ferrocene unit adopts different rotational conformations in the stretched, contracted, and intermediate states in acetone, as shown in Figure 5 and Table 1. We then monitored the C*−Cp−Cp−C* dihedral angle (where C* and Cp denote the substitution position and the center of the two Cp rings of the ferrocene moiety, respectively) in the ferrocene unit. A stepwise alternation of the C*−Cp−Cp−C* dihedral angle was observed from the stretched state (−177.2°) to the contracted state (−112.4°), mediated by the intermediate state (−91.4°) (Figure 5a). Correspondingly, the distance between the two end-capping bis(methoxyl)phenyl groups changed from 32.57 Å in the stretched state to 16.82 Å in the contracted state (Figure 5b), indicative of the stretching/contraction movement of the whole molecular system. The percentage change in molecular length is about 48.4% between the two states, which is much larger than the percentage change (~27%) in human muscle. Moreover, we also monitored the distance between the Fe(II) center and the 9- and 10-sites of the anthracene unit (Figure S7a,b in the Supporting Information and Table 1).

Meanwhile, we have investigated the driving force of the stretching/contraction movement in acetone. We decomposed the interaction energy between the ferrocene-containing dumbbell and the crown ether macrocycle into Coulomb and van der Waals (VDW) contributions, as shown in Figure 5c and Table 1. In the stretched state, the Coulomb interaction energy is as large as −307.9 kJ mol^{-1}, which serves as a primary driving force in comparison with the VDW contribution (−207.1 kJ mol^{-1}). In the contracted state, however, the Coulomb interaction energy is diminished (−142.3 kJ mol^{-1}), indicating a lower affinity between the macrocycle and the triazolium ions. In addition, the VDW contribution significantly increased (−242.9 kJ mol^{-1}) due to the contracted conformation of the dumbbell, where the aromatic units are more tightly packed. In the intermediate state, the Coulomb and VDW interaction energies are comparable, although the Coulomb contribution is slightly larger (Figure S7c, Supporting Information). Therefore, the electrostatic interaction between the crown ether macrocycle and the ammonium ions is mainly responsible for the stretched conformation of the dumbbell under acidic conditions, while the VDW interaction including $\pi-\pi$ and CH−π interactions[18] promotes the contracted conformation of the dumbbell under alkaline conditions. Furthermore, we also have carried out theoretical simulations of different states of the [2](2)rotaxane **1** at 298 K in vacuum for 10 ns; the results also show the same trend in comparison to that in acetone, although it has a much larger percentage change in molecular length and the C*−Cp−Cp−C* dihedral angle in the ferrocene unit (Figures S4−S6 and Table S1, Supporting Information).

CONCLUSION

In conclusion, we have prepared and characterized a novel bistable symmetric [2](2)rotaxane with an anthracene-based

dx.doi.org/10.1021/jo501127h | J. Org. Chem. 2014, 79, 6996−7004

bis(crown ether) as macrocycles and a rotatable ferrocene subunit containing the same rodlike substituents on each side. The system can mimic the stretching and contractional molecular motion performed by skeletal muscle accompanied by a molecular rotary motion in response to external acid−base stimuli, as evidenced by NMR spectroscopic studies and molecular dynamics simulations. The calculated percentage change in molecular length of the [2](2)rotaxane is about 48% in acetone, and the C*−Cp−Cp−C* dihedral angles are computed as −177° in the stretched state and −112° in the contracted state, showing a combination of translational motion and rotary motion in a single-molecule system. Further development of this type of molecular muscle by incorporation into polymeric systems is now under investigation.

EXPERIMENTAL SECTION

General Methods and Materials. ^{1}H NMR, ^{13}C NMR, and 2D ROESY NMR spectra were measured on a AV-400 spectrometer. The electronic spray ionization (ESI) mass spectra were tested on a TOF mass spectrometer. The geometries of the three states of the rotaxane were optimized by density functional theory (DFT) calculations at the BP86/SV(P) level of theory[19] with dispersion correction included by Grimme's model,[20] as implemented in the ORCA program.[21] Starting from the optimized geometries, molecular dynamics (MD) simulations were conducted employing the general Amber force field[16] in combination with the parameters for ferrocene developed by Lopes et al.[17] The partial atomic charges were derived according to the restrained electrostatic potential (RESP) fitting procedure.[22] For each state of the rotaxane, MD simulations were carried out at 298 K in acetone solution with PF_6^- counterions for 10 ns. All solvents were reagent grade and were dried and distilled prior to use according to standard procedures. The molecular structures were confirmed using ^{1}H and ^{13}C NMR spectroscopy and high-resolution ESI mass spectrometry. Compounds **8**−**10** were synthesized and purified according to previous reports.[12a,23]

Synthesis. *Compound* ***7***. TFA (0.90 mL, 12.1 mmol) was added to a solution of **6** (265 mg, 0.24 mmol) in CH_2Cl_2 (10 mL), and the mixture was stirred for 10 h. A saturated aqueous solution of NH_4PF_6 was added to the reaction mixture for 4 h. The organic layer was separated and evaporated under reduced pressure to give a yellow solid, which was dissolved in MeOH (10.0 mL), and a 5.0 mL saturated aqueous solution of NH_4PF_6 was added. After it was stirred for 5 h, the mixture was diluted with CH_2Cl_2 (20 mL) and the organic layer was separated and evaporated under reduced pressure to give the crude product, which was purified by column chromatography (SiO_2, CH_2Cl_2/MeOH 50/1) to afford product **7** (201 mg, 70.0%) as a yellow solid. Mp: 73−75 °C. ^{1}H NMR (CD_3COCD_3, 400 MHz, 298 K): δ 7.65−7.58 (m, 8H), 7.48 (d, J = 8.0 Hz, 4H), 7.00 (d, J = 8.0 Hz, 4H), 5.29 (s, 4H), 4.78 (t, J = 4.0 Hz, 4H), 4.56 (s, 4H), 4.49 (s, 4H), 4.43 (t, J = 4.0 Hz, 4H), 4.24 (d, J = 4.0 Hz, 4H), 4.19−4.17 (m, 4H), 3.87−3.86 (m, 4H), 2.98 (t, J = 4.0 Hz, 2H). ^{13}C NMR (CD_3COCD_3, 100 MHz, 298 K): δ 170.3, 160.8, 139.2, 132.6, 132.4, 131.2, 129.6, 124.3, 115.8, 80.7, 76.1, 73.8, 72.3, 68.9, 68.2, 66.0, 61.1, 58.7, 52.1, 52.0. HRMS (ESI) (m/z): $[M - PF_6]^+$ calcd for $C_{52}H_{54}N_2O_8F_6PFe$, 1035.2871; found, 1035.2909.

Compound ***6***. A mixture of compound **10** (378 mg, 0.89 mmol), 1,1′-ferrocenedicarboxylic acid (**11**; 111.0 mg, 0.40 mmol), 1-(3-(dimethylamino)propyl)-3-ethylcarbodiimide hydrochloride (EDC; 620 mg, 3.2 mmol), and 4-dimethylamiopryidine (DMAP; 98 mg, 0.80 mmol) in CH_2Cl_2 (6.0 mL) was stirred at room temperature overnight under a nitrogen atmosphere. The solution was diluted with 20 mL of CH_2Cl_2 and washed with water (2 × 30 mL), dried over Na_2SO_4, and evaporated under reduced pressure to give the crude product, which was purified by column chromatography (SiO_2, CH_2Cl_2/MeOH 50/1) to afford the product **6** (424 mg, 96.4%) as a red oil. ^{1}H NMR ($CDCl_3$, 400 MHz, 298 K): δ 7.41 (d, J = 8.0 Hz, 4H), 7.24−7.08 (m, 8H), 6.86 (d, J = 8.0 Hz, 4H), 5.24 (s, 4H), 4.81 (t, J = 4.0 Hz, 4H), 4.39−4.23 (m, 16H), 4.14 (t, J = 4.0 Hz, 4H), 3.90 (t, J = 4.0 Hz, 4H), 2.47 (t, J = 4.0 Hz, 2H), 1.48 (s, 18H). ^{13}C NMR ($CDCl_3$, 100 MHz, 298 K): δ 170.3, 158.0, 156.0, 138.3, 135.3, 130.2, 129.4, 128.7, 128.2, 127.6, 114.7, 80.1, 79.5, 74.9, 73.2, 72.6, 71.6, 68.2, 67.2, 65.9, 58.6, 48.7, 48.5, 48.3, 28.5. HRMS (ESI) (m/z): $[M + Na]^+$ calcd for $C_{62}H_{68}N_2O_{12}NaFe$, 1111.4019; found, 1111.4037.

Compound ***5***. A mixture of compound **6** (244 mg, 0.206 mmol), compound **9** (198 mg, 1.02 mmol), and $[Cu(MeCN)_4]PF_6$ (153 mg, 0.410 mmol) was stirred in dry CH_2Cl_2 (5.0 mL) at room temperature under nitrogen for 24 h. After removal of the solvent, the crude product was purified by column chromatography (SiO_2, CH_2Cl_2/MeOH 100/1) to afford product **5** (234 mg, 77.0%) as a yellow solid. Mp: 68−70 °C. ^{1}H NMR (CD_3COCD_3, 400 MHz, 298 K): δ 7.95 (s, 2H), 7.50 (d, J = 8.0 Hz, 4H), 7.34−7.26 (m, 4H), 7.19−7.11 (m, 4H), 6.87 (d, J = 8.0 Hz, 4H), 6.51 (d, J = 4.0 Hz, 4H), 6.45 (t, J = 4.0 Hz, 2H), 5.53(s, 4H), 5.25(s, 4H), 4.76 (t, J = 4.0 Hz, 4H), 4.65 (s, 4H), 4.39−4.26 (m, 12H), 4.10 (t, J = 4.0 Hz, 4H), 3.83 (t, J = 4.0 Hz, 4H), 3.75 (s, 12H), 1.46 (s, 18H). ^{13}C NMR (CD_3COCD_3, 100 MHz, 298 K): δ 170.3, 162.2, 159.2, 156.3, 139.5, 139.1, 136.6, 131.2, 129.6, 115.3, 106.9, 100.6, 80.1, 73.9, 73.7, 72.3, 69.4, 68.2, 66.3, 65.2, 55.7, 54.2, 28.6. HRMS (ESI) (m/z): $[M + H]^+$ calcd for $C_{80}H_{91}N_8O_{16}Fe$, 1475.5902; found, 1475.5978; $[M + Na]^+$ calcd for $C_{80}H_{90}N_8O_{16}NaFe$, 1497.5722; found, 1497.5848; $[M + K]^+$ calcd for $C_{80}H_{90}N_8O_{16}KFe$, 1513.5461; found, 1513.5570.

Compound ***4***. Compound **5** (212 mg, 0.144 mmol) was dissolved in iodomethane (2.0 mL) and $CHCl_3$ (2.0 mL), and then the mixture was stirred for 2 days at 40 °C. The solvent was removed, the residue was dissolved in MeOH (10.0 mL), and 4.0 mL of a saturated aqueous solution of NH_4PF_6 was added. After it was stirred for 5 h, the mixture was diluted with CH_2Cl_2 (20 mL) and the organic layer was separated and washed with deionized water and then evaporated under reduced pressure to give the crude product, which was purified by column chromatography (SiO_2, CH_2Cl_2/MeOH 50/1) to give product **4** (164 mg, 63.5%) as a yellow solid. Mp: 77−79 °C. ^{1}H NMR (CD_3COCD_3, 400 MHz, 298 K): δ 8.89 (s, 2H), 7.51 (d, J = 8.0 Hz, 4H), 7.34−7.28 (m, 4H), 7.18 (d, J = 8.0 Hz, 4H), 6.88 (d, J = 8.0 Hz, 4H), 6.70 (d, J = 4.0 Hz, 4H), 6.58 (t, J = 4.0 Hz, 2H), 5.89 (s, 4H), 5.26 (s, 4H), 5.07 (s, 4H), 4.77 (t, J = 4.0 Hz, 4H), 4.48 (s, 6H), 4.38−4.27 (m, 12H), 4.20−4.18 (m, 4H), 4.01−3.99 (m, 4H), 3.80 (s, 12H), 1.46 (s, 18H). ^{13}C NMR (CD_3COCD_3, 100 MHz, 298 K): δ 170.3, 162.5, 158.9, 156.3, 142.2, 136.7, 135.2, 131.6, 130.3, 129.6, 115.3, 108.1, 101.6, 80.2, 73.9, 73.8, 72.3, 70.6, 67.9, 66.3, 61.4, 57.9, 55.9, 39.1, 28.6. HRMS (ESI) (m/z): $[M - PF_6]^+$ calcd for $C_{82}H_{96}N_8O_{16}F_6PFe$, 1649.5936; found, 1649.6105.

Compound ***3***. TFA (0.30 mL, 3.59 mmol) was added to a solution of **4** (129 mg, 0.072 mmol) in CH_2Cl_2 (10 mL), and the mixture was stirred for 10 h. A saturated aqueous solution of NH_4PF_6 was added to the reaction mixture for 4 h. The organic layer was separated and evaporated under reduced pressure to give a yellow solid, which was dissolved in MeOH (10.0 mL), and to this solution was added 5.0 mL of a saturated aqueous solution of NH_4PF_6. After it was stirred for 5 h, the mixture was diluted with CH_2Cl_2 (10 mL), and the organic layer was separated and evaporated under reduced pressure to give the crude product, which was purified by column chromatography (SiO_2, CH_2Cl_2/MeOH 30/1) to afford product **3** (115.3 mg, 85.0%) as a yellow solid. Mp: 73−75 °C. ^{1}H NMR (CD_3CN, 400 MHz, 298 K): δ 8.32 (s, 2H), 7.55 (d, J = 8.0 Hz, 4H), 7.48 (d, J = 8.0 Hz, 4H), 7.37 (d, J = 8.0 Hz, 4H), 6.94 (d, J = 8.0 Hz, 4H), 6.60 (d, J = 4.0 Hz, 4H), 6.57 (t, J = 4.0 Hz, 2H), 5.62 (s, 4H), 5.27 (s, 4H), 4.81 (s, 4H), 4.78 (t, J = 4.0 Hz, 4H), 4.42 (t, J = 4.0 Hz, 4H), 4.22 (s, 6H), 4.18−4.16 (m, 4H), 4.12 (s, 4H), 4.07 (s, 4H), 3.91−3.89 (m, 4H), 3.80 (s, 12H). ^{13}C NMR (CD_3CN, 100 MHz, 298 K): δ 170.7, 162.5, 160.2, 141.9, 138.8, 135.0, 133.4, 132.5, 131.0, 130.1, 129.6, 125.7, 115.7, 108.1, 101.8, 74.0, 73.7, 72.4, 70.5, 68.1, 66.3, 61.3, 57.9, 56.3, 52.1, 39.4. HRMS (ESI) (m/z): $[M - PF_6]^+$ calcd for $C_{72}H_{82}N_8O_{12}F_{18}P_3Fe$, 1741.4327; found, 1741.4326.

Compound ***2***. A mixture of **7** (141 mg, 0.12 mmol) and crown ether **8** (120 mg, 0.12 mmol) was stirred for 30 min in dry CH_2Cl_2 (3 mL) at room temperature. After **9** (115 mg, 0.60 mmol) and $[Cu(CH_3CN)_4]PF_6$ (89 mg, 0.24 mmol) were added to the solution, the mixture was stirred for 2 days. After removal of the solvent, the

dx.doi.org/10.1021/jo501127h | J. Org. Chem. 2014, 79, 6996−7004

residue was purified by column chromatography (SiO_2, CH_2Cl_2/MeOH 50/1) to afford product **2** (128 mg, 41.7%) as a yellow solid. Mp: 92−94 °C. ^{1}H NMR (CD_3COCD_3, 400 MHz, 298 K): δ 7.95 (s, 2H), 7.60 (d, J = 8.0 Hz, 4H), 7.38 (d, J = 8.0 Hz, 4H), 7.31 (s, 4H), 7.03 (d, J = 8.0 Hz, 4H), 6.95−6.90 (m, 8H), 6.86−6.82 (m, 4H), 6.50 (d, J = 4.0 Hz, 4H), 6.44 (t, J = 4.0 Hz, 2H), 5.53 (s, 4H), 4.89−4.83 (m, 8H), 4.61 (s, 8H), 4.52−4.46 (m, 8H), 4.28 (t, J = 4.0 Hz, 4H), 4.26−4.22 (m, 6H), 4.20−4.15 (m, 6H), 4.07−4.03 (m, 6H), 4.0 (t, J = 4.0 Hz, 8H), 3.92−3.87 (m, 10H), 3.86−3.82 (m, 4H), 3.79−3.77 (m, 8H), 3.74 (s, 12H), 3.73−3.70 (m, 4H), 3.38 (t, J = 8.0 Hz, 4H), 1.80 (q, J = 16.0 Hz, 4H), 1.10 (t, J = 8.0 Hz, 6H). ^{13}C NMR (CD_3COCD_3, 100 MHz, 298 K): δ 169.6, 162.2, 160.5, 148.7, 148.0, 139.1, 138.1, 132.6, 131.9, 130.4, 130.3, 128.8, 126.3, 125.3, 122.0, 115.6, 113.3, 106.9, 104.7, 100.5, 73.9, 73.2, 71.9, 71.5, 71.4, 71.0, 69.3, 68.8, 68.7, 68.2, 65.6, 55.7, 54.3, 53.0, 52.9, 24.6, 15.0. HRMS (ESI) (m/z): $[M - 2PF_6]^{2+}$ calcd for $C_{126}H_{150}N_8O_{28}Fe/2$, 1139.4954; found, 1139.4958.

Compound **1**. Rotaxane **2** (81 mg, 0.032 mmol) was dissolved in iodomethane (2.0 mL) and $CHCl_3$ (2.0 mL), and then the mixture was stirred for 4 days at 40 °C. The solvent was removed, the residue was dissolved in acetone (5.0 mL), and 5.0 mL of a saturated aqueous solution of NH_4PF_6 was added. After it was stirred for 10 h, the mixture was diluted with CH_2Cl_2 (10 mL) and the organic layer was separated, washed with deionized water, and then evaporated under reduced pressure to give the crude product, which was purified by column chromatography (SiO_2, CH_2Cl_2/MeOH 50/1) to give product **1** (58.3 mg, 64.0%) as a yellow solid. Mp: 111−113 °C. ^{1}H NMR (CD_3COCD_3, 400 MHz, 298 K): δ 8.84 (s, 2H), 7.62 (d, J = 8.0 Hz, 4H), 7.38 (d, J = 8.0 Hz, 4H), 7.32 (s, 4H), 7.03 (d, J = 8.0 Hz, 4H), 6.98 (d, J = 8.0 Hz, 4H), 6.93−6.91 (m, 4H), 6.86−6.82 (m, 4H), 6.69 (d, J = 4.0 Hz, 4H), 6.56 (t, J = 4.0 Hz, 2H), 5.87 (s, 4H), 5.04 (s, 4H), 4.90−4.84 (m, 8H), 4.58 (s, 4H), 4.54−4.49 (m, 8H), 4.45 (s, 6H), 4.29 (t, J = 4.0 Hz, 4H), 4.26−4.22 (m, 6H), 4.18−4.15 (m, 6H), 4.07−3.84 (m, 36H), 3.78 (s, 12H), 3.74−3.70 (m, 4H), 3.38 (t, J = 4.0 Hz, 4H), 1.79 (q, J = 16.0 Hz, 4H), 1.10 (t, J = 8.0 Hz, 6H). ^{13}C NMR (CD_3COCD_3, 100 MHz, 298 K): δ 169.5, 162.8, 160.3, 148.7, 148.0, 142.1, 138.1, 135.2, 133.4, 132.0, 130.4, 130.3, 128.9, 126.3, 122.0, 115.6, 113.3, 108.0, 104.7, 101.6, 73.9, 73.1, 71.9, 71.5, 71.4, 71.0, 68.8, 68.7, 67.9, 65.7, 61.3, 57.9, 55.9, 39.1, 32.6, 31.7, 24.6, 23.3, 22.3, 15.0, 14.4. HRMS (ESI) (m/z): $[M - 2PF_6]^{2+}$ calcd for $C_{128}H_{156}N_8O_{28}FeP_2F_{12}/2$, 1299.4813; found, 1299.4982; $[M - 3PF_6]^{3+}$ calcd for $C_{128}H_{156}N_8O_{28}FePF_6/3$, 818.0007; found, 818.0011; $[M - 4PF_6]^{4+}$ calcd for $C_{128}H_{156}N_8O_{28}Fe/4$, 577.2795; found, 577.2604.

■ ASSOCIATED CONTENT

Supporting Information

Text, figures, and a table giving full experimental procedures and characterization data of all compounds, including ^{1}H NMR and ^{13}C NMR spectroscopy and HR-ESI spectrometry, and molecular dynamics simulations results. This material is available free of charge via the Internet at http://pubs.acs.org.

■ AUTHOR INFORMATION

Corresponding Author

*D.-H.Q.: fax, +86-21 64252288; e-mail, dahui_qu@ecust.edu.cn.

Notes

The authors declare no competing financial interest.

■ ACKNOWLEDGMENTS

We thank the NSFC/China (21272073, 21190033), the National Basic Research 973 Program (2011CB808400), the Fundamental Research Funds for the Central Universities, the Innovation Program of Shanghai Municipal Education Commission, and the Scientific Research Foundation for the Returned Overseas Chinese Scholars, State Education Ministry, for financial support. The authors thank Dr. Gábor London from the University of Szeged for helpful discussions.

■ REFERENCES

(1) (a) Saha, S.; Stoddart, J. F. *Chem. Soc. Rev.* **2007**, *36*, 77−92. (b) Mateo-Alonso, A. *Chem. Commun.* **2010**, *46*, 9089−9099. (c) Sauvage, J.-P.; Gaspard, P.; Balzani, V.; Credi, A.; Venturi, M. *Molecular Machines Based on Rotaxanes and Catenanes*; Wiley-VCH: Weinheim, Germany, 2010. (d) Feringa, B. L.; Browne, W. R. *Molecular Switches*; Wiley-VCH: Weinheim, Germany, 2011. (e) Dasgupta, S.; Wu, J.-S. *Chem. Sci.* **2012**, *3*, 425−432. (f) Zhang, M.-M.; Zhu, K.-L.; Huang, F.-H. *Molecular Devices: Molecular Machinery*; Wiley-VCH: Weinheim, Germany, 2012.

(2) (a) Champin, B.; Mobian, P.; Sauvage, J.-P. *Chem. Soc. Rev.* **2007**, *36*, 358−366. (b) Mullen, K. M.; Beer, P. D. *Chem. Soc. Rev.* **2009**, *38*, 1701−1713. (c) Balzani, V.; Credi, A.; Venturi, M. *Chem. Soc. Rev.* **2009**, *38*, 1542−1550.

(3) (a) Kinbara, K.; Aida, T. *Chem. Rev.* **2005**, *105*, 1377−1400. (b) Kay, E. R.; Leigh, D. A.; Zerbetto, F. *Angew. Chem., Int. Ed.* **2007**, *46*, 72−191. (c) Chen, K. Y.; Ivashenko, O.; Carroll, G. T.; Robertus, J.; Kistemaker, J. C. M.; London, G.; Browne, W. R.; Rudolf, P.; Feringa, B. L. *J. Am. Chem. Soc.* **2014**, *136*, 3219−3224.

(4) (a) Carroll, G. T.; Pollard, M. M.; Deldena, R.; Feringa, B. L. *Chem. Sci.* **2010**, *1*, 97−101. (b) Cnossen, A.; Hou, L.-L.; Pollard, M. M.; Wesenhagen, P. V.; Browne, W. R.; Feringa, B. L. *J. Am. Chem. Soc.* **2012**, *134*, 17613−17619. (c) Filatov, M.; Olivucci, M. *J. Org. Chem.* **2014**, *79*, 3587−3600.

(5) (a) Chuang, C.-J.; Li, W.-S.; Lai, C.-C.; Liu, Y.-H.; Peng, S.-M.; Chao, I.; Chiu, S.-H. *Org. Lett.* **2009**, *11*, 385−388. (b) Du, G.-Y.; Moulin, E.; Jouault, N.; Buhler, E.; Giuseppone, N. *Angew. Chem., Int. Ed.* **2012**, *51*, 12504−12508. (c) Bruns, C. J.; Stoddart, J. F. *Nat. Nanotechnol.* **2013**, *8*, 9−10.

(6) (a) Qu, D.-H.; Tian, H. *Chem. Sci.* **2011**, *2*, 1011−1015. (b) Zhu, L.-L.; Yan, H.; Nguyen, K. T.; Tian, H.; Zhao, Y.-L. *Chem. Commun.* **2012**, *48*, 4290−4292. (c) Dzyuba, E. V.; Baytekin, B.; Sattler, D.; Schalley, C. A. *Chem. Eur. J.* **2012**, *6*, 1171−1175.

(7) (a) Qu, D.-H.; Wang, Q.-C.; Tian, H. *Angew. Chem., Int. Ed.* **2005**, *44*, 5296−5299. (b) Saha, S.; Flood, A. H.; Stoddart, J. F.; Impellizzeri, S.; Silvi, S.; Venturi, M.; Credi, A. *J. Am. Chem. Soc.* **2007**, *129*, 12159−12171. (c) Zhou, W.-D.; Chen, D.-G.; Li, J.-B.; Xu, J.-L.; Lv, J.; Liu, H.-B.; Li, Y.-L. *Org. Lett.* **2007**, *9*, 3929−3932. (d) Coskun, A.; Friedman, D. C.; Li, H.; Patel, K.; Khatib, H. A.; Stoddart, J. F. *J. Am. Chem. Soc.* **2009**, *131*, 2493−2495. (e) Zhang, H.; Hu, J.; Qu, D.-H. *Org. Lett.* **2012**, *14*, 2334−2337. (f) Zhu, L.-L.; Yan, H.; Wang, X.-J.; Zhao, Y.-L. *J. Org. Chem.* **2012**, *77*, 10168−10175. (g) Zhang, J.-N.; Li, H.; Zhou, W.; Yu, S.-L.; Qu, D.-H.; Tian, H. *Chem. Eur. J.* **2013**, *19*, 17192−17200.

(8) (a) Badjic, J. D.; Balzani, V.; Credi, A.; Silvi, S.; Stoddart, J. F. *Science* **2004**, *303*, 1845−1849. (b) Badjic, J. D.; Ronconi, C. M.; Stoddart, J. F.; Balzani, V.; Silvi, S.; Credi, A. *J. Am. Chem. Soc.* **2006**, *128*, 1489−1499. (c) Zhang, Z.-J.; Han, M.; Zhang, H.-Y.; Liu, Y. *Org. Lett.* **2013**, *15*, 1698−1701.

(9) (a) Alvarez-Pérez, M.; Goldup, S. M.; Leigh, D. A.; Slawin, A. M. Z. *J. Am. Chem. Soc.* **2008**, *130*, 1836−1838. (b) Carlone, A.; Goldup, S. M.; Lebrasseur, N.; Leigh, D. A.; Wilson, A. J. *Am. Chem. Soc.* **2012**, *134*, 8321−8323.

(10) (a) Lavella, G. J.; Jadhav, A. D.; Maharbiz, M. M. *Nano Lett.* **2012**, *12*, 4983−4987. (b) Qu, D.-H.; Tian, H. *Chem. Sci.* **2013**, *4*, 3031−3035.

(11) Ma, Y.-X.; Meng, Z.; Chen, C.-F. *Org. Lett.* **2014**, *16*, 1860−1863.

(12) (a) Jiang, W.; Han, M.; Zhang, H.-Y.; Zhang, Z.-J.; Liu, Y. *Chem. Eur. J.* **2009**, *15*, 9938−9945. (b) Zhang, Z.-J.; Han, M.; Zhang, H.-Y.; Liu, Y. *Org. Lett.* **2013**, *15*, 1698−1701.

(13) (a) Zhang, D.; Zhang, Q.; Sua, J.-H.; Tian, H. *Chem. Commun.* **2009**, 1700−1702. (b) Iordache, A.; Oltean, M.; Milet, A.; Thomas, F.; Baptiste, B.; Saint-Aman, E.; Bucher, C. *J. Am. Chem. Soc.* **2012**, *134*, 2653−2671.

(14) (a) Jiang, Y.; Guo, J.-B.; Chen, C.-F. *Org. Lett.* **2010**, *12*, 4248−4251. (b) Clavel, C.; Romuald, C.; Brabet, E.; Coutrot, F. *Chem.−Eur. J.* **2013**, *19*, 2982−2989. (c) Zhou, W.; Guo, Y.-J.; Qu, D.-H. *J. Org.*

Chem. **2013**, *78*, 590−596. (d) Li, H.; Zhang, J.-N.; Zhou, W.; Zhang, H.; Zhang, Q.; Qu, D.-H.; Tian, H. *Org. Lett.* **2013**, *15*, 3070−3073.
(15) (a) Hänni, K. D.; Leigh, D. A. *Chem. Soc. Rev.* **2010**, *39*, 1240−1251. (b) Zhang, H.; Kou, X.-X.; Zhang, Q.; Qu, D.-H.; Tian, H. *Org. Biomol. Chem.* **2011**, *9*, 4051−4056. (c) Zhang, H.; Zhou, B.; Li, H.; Qu, D.-H.; Tian, H. *J. Org. Chem.* **2013**, *78*, 2091−2098. (d) Zhou, W.; Zhang, H.; Li, H.; Zhang, Y.; Wang, Q.-C.; Qu, D.-H. *Tetrahedron* **2013**, *69*, 5319−5325. (e) Zhou, W.; Wu, Y.; Zhai, B.-Q.; Wang, Q.-C.; Qu, D.-H. *RSC Adv.* **2014**, *4*, 5148−5151.
(16) Wang, J.; Wolf, R. M.; Caldwell, J. W.; Kollman, P. A.; Case, D. A. *J. Comput. Chem.* **2004**, *25*, 1157−1174.
(17) Lopes, J. N. C.; do Couto, P. C.; da Piedade, M. E. M. *J. Phys. Chem. A* **2006**, *110*, 13850−13856.
(18) Kim, E.; Paliwal, S.; Wilcox, C. S. *J. Am. Chem. Soc.* **1998**, *120*, 11192−11193.
(19) (a) Becke, A. D. *Phys. Rev. A* **1988**, *38*, 3098−3100. (b) Perdew, J. P. *Phys. Rev. B* **1986**, *33*, 8822−8824. (c) Schaefer, A.; Horn, H.; Ahlrichs, R. *J. Chem. Phys.* **1992**, *97*, 2571.
(20) Grimme, S. *J. Comput. Chem.* **2006**, *27*, 1787−1799.
(21) Neese, F. *WIREs Comput. Mol. Sci.* **2012**, *2*, 73−78.
(22) Bayly, C. I.; Cieplak, P.; Cornell, W.; Kollman, P. A. *J. Phys. Chem.* **1993**, *97*, 10269−10280.
(23) Li, H.; Zhang, H.; Zhang, Q.; Zhang, Q.-W.; Qu, D.-H. *Org. Lett.* **2012**, *14*, 5900−5903.